American Journal of Materials Engineering and Technology, 2020, Vol. 8, No. 1, 9-17
Available online at http://pubs.sciepub.com/materials/8/1/2
Published by Science and Education Publishing
DOI:10.12691/materials-8-1-2

Shape Optimization Study on Composite Material Using Finite Element Analysis

Adisa O. Akinbode*, Prof Anjali DeSilva

Department of Mechanical Engineering, SCEBE, Glasgow Caledonian University, Glasgow, UK
*Corresponding author: adisa.akinbode@amcsgroup.com

Received October 12, 2020; Revised November 13, 2020; Accepted November 20, 2020

Abstract This study attempts to improve the use of composite materials in engineering applications through shape optimization by adopted finite element analysis (FEA) tools and regression models. SolidWorks was used to develop the geometries, ANSYS was used for the FEA, while MATLAB was used for the regression analysis. The equivalent stress, equivalent strain, and total deformation on the material for different shapes and configurations was studied. Circular shape and dog bone, both without holes were the shapes considered as initial or primary configuration. The optimal behavior predicted for the circular shape specimen suggest that staggered arrangement, 8 holes, 3 or 6 layers of plate combined, and circular holes will be the required combination for best performance. This deduction was made based on the prediction by the model selected for regression analysis. In the case of dog bone shape, no hole, single hole, and multiple holes were considered. It was observed that multiple (5) holes with 5 mm will significantly increase the equivalent stress and equivalent strain on the specimen, while no significant change was observed for the total deformation.

Keywords: *composites, shape optimization, finite element analysis, machine learning*

Cite This Article: Adisa O. Akinbode, and Prof Anjali DeSilva, "Shape Optimization Study on Composite Material Using Finite Element Analysis." *American Journal of Materials Engineering and Technology*, vol. 8, no. 1 (2020): 9-17. doi: 10.12691/materials-8-1-2.

1. Introduction

Composites are turning out to be in very high demand in engineering applications. This is mostly due to their comparatively high strength-to-weight ratio obtained from the ingenious combination of complimentary, naturally occurring (or easily synthesized) materials that have come to be known as fiber and resin, bonded in a matrix [1]. Applications in this regard include automobile turbines, bumpers, fuel injection parts, and many more [2]. Other novel and emerging applications include aircraft parts, cowlings, and even full wings [3]. This is a kind of departure from the conventional metal sheets which as it turns out are heavier and relatively less desirable in a weight sensitive application such as air travel. A key parameter here is the volume of fuel consumed in air transport. And these being a critical design consideration, airliners are increasingly taking on more composite parts. Another area of desirable behavior is impact resistance. As a result, racing vehicles and other impact-prone vehicles are adopting more composite parts. This is in addition to the lightweight advantages of using composite rather than metal/alloy parts [4]. In addition to the foregoing, manufacturing considerations also favor the use of composites in the sense that they are readily formable and do not require as much processing to get the final shape. This in a way provides the opportunity to experiment with different fiber-resin combinations for different properties required in various applications. This is evident in the fact that several property sets have been documented for the same fiber-resin mix. However, it is also as a result of this that the standardization of composite properties is relatively difficult, as several parameter combinations are possible/readily available.

There are defects which exist due to manufacturing process or procedure. Such defects cause the composite properties to depart from the expectations or design specifications. These defects are summarized as: thickness of composite materials, fiber volume fraction and void property. Another important factor to be considered is the damage caused on composite which occur after composite is loaded. Damage is studied after putting into consideration all the defects arising from manufacturing. Study on adhesive joints, when two materials of the composite are joined, had been earlier studied in the works of [5,6]. Different types of joint could be studied, e.g. single-lap joint, wavy-lap joint, butt-joint, etc. Finite element analysis is then carried out to understand the stress field distribution on the joints, thereby making it easy to conclude on which type of joint is suitable with respect to other features on the composite material. Numerical simulation analyses of single lap joints for wood powder/polyethylene (WP/PE) composites formed with epoxy and acrylic ester adhesives was conducted by Zhou and Di [7]. The finite element model of the single lap bonded joints of WP/PE was established through the

elastic-plastic finite element method, and the influences of adhesive and lap length on the stress distribution in the adhesive joints were analyzed.

Beyond the strength-to-weight ratio, stiffness and toughness/impact resistance, another area that is of interest to engineers is flexural rigidity or resistance to cyclic loading [8]. This becomes particularly important in applications such as aircraft wings which are constantly in a condition of twist due to load reversals largely induced by air turbulence and vehicle maneuvering [9,10]. Other applications subject to identical loading conditions include turbine blades, ship hulls [11]; high speed marine vehicles and even connections adopted in marine superstructures [12].

The idea of improving the performance of say, aircrafts is fundamentally associated with weight reduction. The benefits herewith accruable include minimizing fuel consumption (and the attendant environmental impact reduction), drag reduction, reduced cost of operation and increased maneuverability. As a result, weight reduction shall be the focus this research with respect to the application of composites in fatigue/cyclically loaded environments. This work will sample different weight reduction approaches within the context of geometric variation, to obtain the optimal parameter combination in this regard that tends toward the most desirable weight reduction configuration. This will of course be considered in terms of mechanical response of the composite material, examined under different physical and geometric parameter variations to determine the best combination of configurations that minimizes a weight and flexural stress.

2. Methodology

In this study, two configurations of the selected composite as the specimen will be considered. For the first configuration, a circular shape considered. Circular shape is chosen because the shape eliminates the issues associated with stress concentration at corners/extremities, which a circle does not have. To account for increase in strength and rigidity, the number of composite layers used in this loading condition was varied across the entire experiment. This variation of layers constitutes the first level of complexity introduced in this study. Another level of complexity included is with respect to 'holes' placed across the plain surface of the composite plates. There are three levels of variation possible with these holes. These are: the shape of the hole, the number of holes and the alignment in each case. For the second configuration the "dog bone" shape was considered which the standard shape is recommended for mechanical strength analysis of materials. The dimensions were based on ASTM E8 Standard. Variation of holes was also considered in the dog bone shape, but in this case, effect of increase in the diameter of the hole and increase in the number of holes on the material was investigated. For the single hole, the origin of the circle is at the center point at the top surface of the specimen, while for multiple holes (5 holes), two more holes were created each on the positive and negative direction of the x-axis to make a total of five holes. The distance between two holes is 1 mm, and this was the same for all diameter of holes considered in the study. This gives a fundamental idea of what this study seeks to accomplish, namely the best approach to material reduction that justifies safe and effective weight minimization in composite applications.

2.1. Physical Models

For geometry development and assembly, SolidWorks was used. As a Computer Aided Design package, it was used to generate the shapes in their various configurations and specifying the basic relationship between several parts in areas where more than one part is used (this feature was generally adopted in the development of multi-layered configurations). Having developed the desired geometry, it was exported in a compatible file format as an input to the FEA tool, namely ANSYS Mechanical. The FEA environment provides the tools for material assignment, meshing, specifying boundary conditions, load application, specifying analysis hyper-parameters, and engaging the simulation engine such that one can tweak the analysis settings as the problem may require. The primary responses obtained from the FEA tool include: the stress, strain, and the deformation. The tool also has a Graphic User Interface (GUI) where the stress/strain/deformation distribution throughout the specimen are displayed. This information, in addition to the critical points (points of maximum stress/strain/deformation) combines to give a powerful framework where useful deductions can be made to describe and predict the behavior of the specimen. The results from the simulation were normalized and integrated into a framework of derived functions that were fed into a Machine Learning (ML) framework in MATLAB. MATLAB provides a structure for the deployment of ML algorithms for trend identification, regression, and data fitting. This is especially useful where multiple factors are involved. The regression behavior was subsequently observed and used to stipulate the overall design approach to this kind of design study, toward the predetermined objective. All the shapes and different configurations considered for this study are presented in Figure 1 to Figure 8.

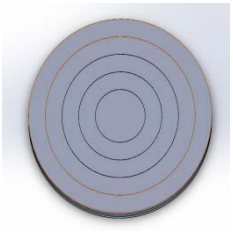

Figure 1. Plane, no holes, 3 plates

Figure 2. Four holes, single plate, round shape

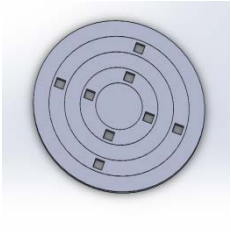

Figure 3. 8 holes, single plate, square shape, aligned

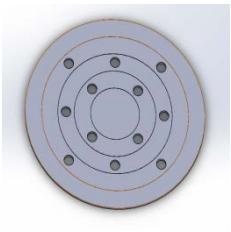

Figure 4. 12 holes, single plate, circular

Figure 5. Single hole, six plates, double elliptical shape

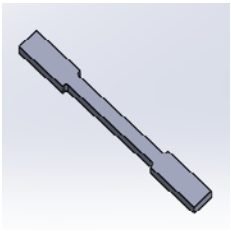

Figure 6. Plain Dog bone shape

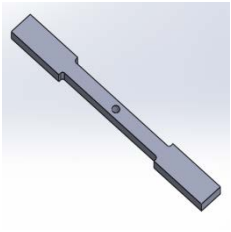

Figure 7. Dog bone shape with single hole

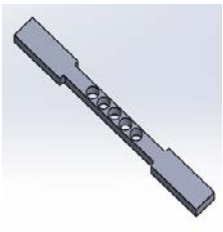

Figure 8. Dog bone shape with five holes

2.2. Simulation Procedure

This set up considered in ANSYS Mechanical primarily concerned with the mechanical response (stress, strain, and deformation) shall only consider the Static Structural module. The material adopted for this study is carbon fiber reinforced epoxy matrix. This is an aircraft-grade material with application in other sensitive areas of engineering (Srikaris, ATSB Aust, Hayley Birch@end, R. Das). The specific properties of the type used in this study are presented in Table 1. The Material is generally described as an Epoxy_Carbon_Woven_395GPa_Prepreg.

Table 1. Properties of the variation of Epoxy Carbon used

Property	Value	Unit
Density	1.48E-09	kg/m^3
Young's Modulus X direction	91820	MPa
Young's Modulus Y direction	91820	MPa
Young's Modulus Z direction	9000	MPa
Poisson's Ratio XY	0.05	
Poisson's Ratio YZ	0.3	
Poisson's Ratio YZ	0.3	
Shear Modulus XY	19500	MPa
Shear Modulus YZ	3000	MPa
Shear Modulus XZ	3000	MPa
Coefficient of Thermal Expansion		
Coefficient of Thermal Expansion X Direction	2.5E-06	
Coefficient of Thermal Expansion Y Direction	2.5E-06	
Coefficient of Thermal Expansion Z Direction	1E-06	
Orthotropic Stress Limits		
Tensile X Direction	829	MPa
Tensile Y Direction	829	MPa
Tensile Z Direction	50	MPa
Compressive X Direction	-439	MPa
Compressive Y Direction	-439	MPa
Compressive Z Direction	-140	MPa
Shear XY	120	MPa
Shear YZ	50	MPa
Shear XZ	50	MPa
Orthotropic Strain Limits		
Tensile X Direction	0.0086	
Tensile Y Direction	0.0086	
Tensile Z Direction	0.0086	
Compressive X Direction	-0.0055	
Compressive Y Direction	-0.0055	
Compressive Z Direction	-0.0055	
Shear XY	0.018	
Shear YZ	0.012	
Shear XZ	0.018	

2.2.1. Mesh Generation

Meshing entails the discretization of the geometric domain in preparation for solution by numerical methods. A typical Finite Element Analysis (FEA) tool is essentially built on this function. In fact, the concept of finite elements derives its recognition and practical application from meshing. The discretization in *meshing* is really dividing the problem domain (geometry) into *discrete elements* wherein the governing equations can be locally solved before being integrated (considering the boundary conditions) into the global system of solutions. The meshing method affects two principal factors, namely - the computation time and the accuracy, and these generally in an inverse order. The types of physics being solved for and the complexity of the geometry/problem domain also affects the *degree of fineness* required for a

particular study. It should also not go without saying that the hardware capacity in terms of processing power will determine if a computer can handle a problem efficiently or not at all. For this study, a medium tetrahedral mesh adjusted for edge conditions and smoothing was applied across the geometries in this study. Two examples showing the generated mesh of circular configuration and dog bone configuration are presented in Figure 9 and Figure 10 respectively.

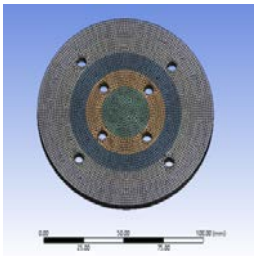

Figure 9. Circular configuration mesh

Figure 10. Dog bone configuration mesh

2.2.2. Boundary Conditions

The boundary conditions constitute the imposed loads and physical restrictions applied to the geometry. The way these are applied is based on the kind of physics or operational condition we are trying to simulate. In this case, we are concerned with fatigue loading and this is implemented in such a way that load reversal occurs every second, beginning at the center of the specimen and progressively to its outer reaches. The geometry itself was assembled in such a way that load transition boundaries may be defined at each instance of loading. The way this works is that the pressure load of *5Mpa* magnitude is applied first at the center surface (first load section) in one direction while the other load sections at kept at *0Mpa* in the first analysis cycle. In the next cycle, the load shifts to the next load section (concentric to the first) while others are kept at zero, including the first. This is done sequentially from inside out (a gif file is attached in this regard to show this loading progression) for the entire analysis time, numbering up to five load sections. In addition to the load, the circular (peripheral) edge of each geometry was fixed throughout the simulation. The loading described is specific to circular configuration and a sample is illustrated in Figure 11. For the dog bone configuration, the analysis of the entire sides of the specimen is assumed to be fixed, hence it is assigned to be fixed, while varying pressure is applied on the entire top surface of the specimen. Figure 12 shows the sample of a specimen with the fixed sides and the face under pressure impact.

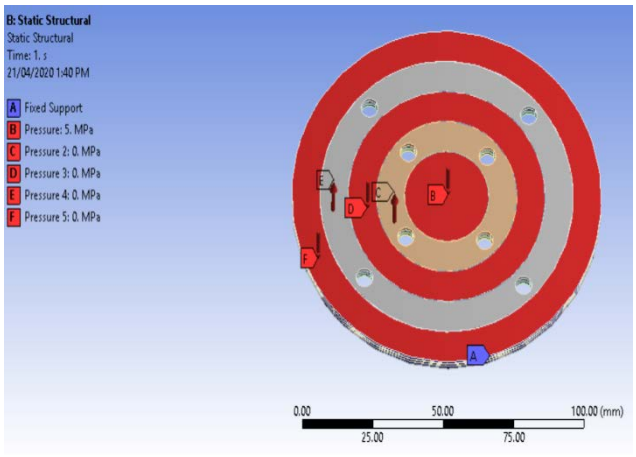

Figure 11. Boundary conditions for circular shape

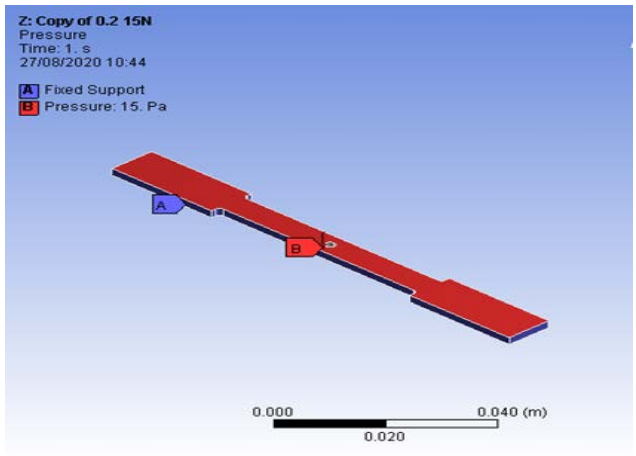

Figure 12. Boundary conditions for dog bone shape

3. Result and Discussions

The solutions of interest as defined earlier are the stress, strain, and deformation. The parameters specified for solution specification are the force convergence and the Newton-Raphson error. Firstly, the results obtained based on GUI rendition are shown in Figure 13 - Figure 15 of a specific configurations for the circular shape.

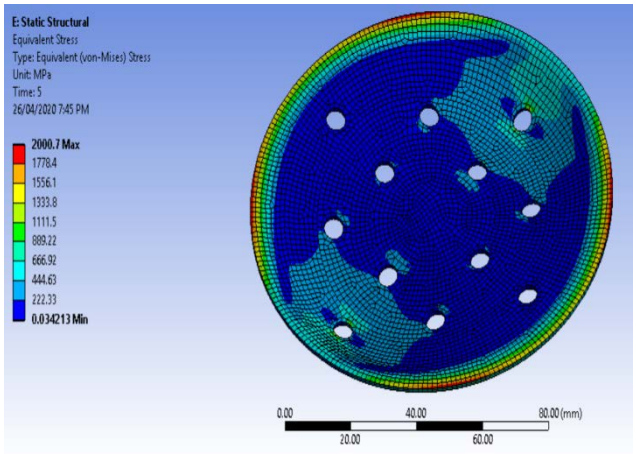

Figure 13. Stress information

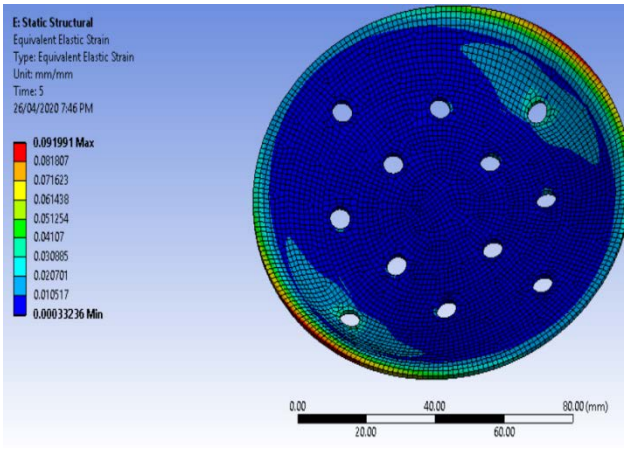

Figure 14. Strain information

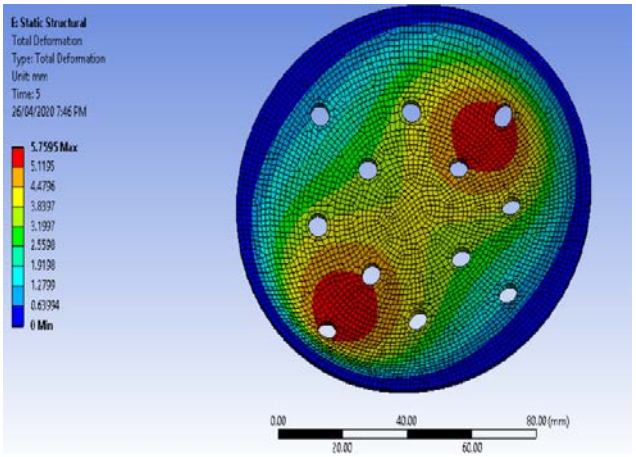

Figure 15. Deformation information

To capture the full objective of this study, the raw results of the FEA tool will not be sufficient. In other words, just stress, strain and deformation have a limited application when it comes to transcendental objectives such as limiting stress concentration and weight minimization. In this regard, the stress pattern and the distribution of deformation between any given piece is hardly identical. Therefore, quantifying this information numerically provides a framework for the extended application of the simulation results. As shown in Figure 16 and Figure 17, though the stress values may be somewhat close (as it turns out to be in certain instances), the stress pattern, deformation distribution and the position of maximum are usually different. As a result, derived metrics were developed to capture and extend the capacity of this research to capture the said objectives.

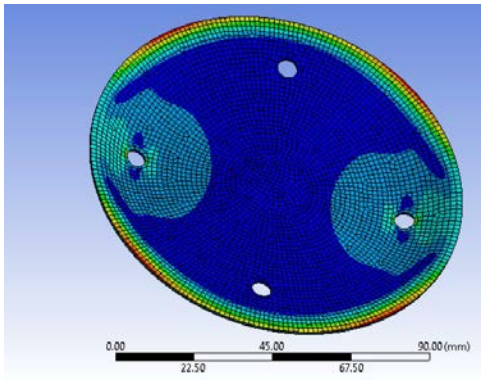

Figure 16. Stress distribution for one configuration

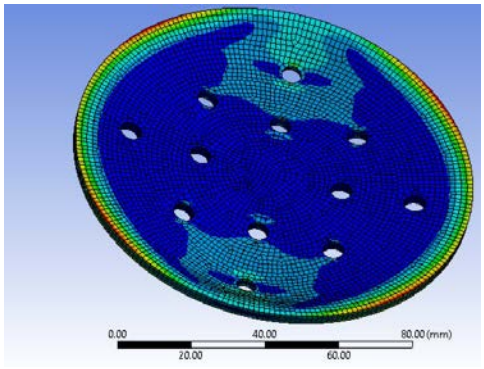

Figure 17. Stress distribution for another configuration

Based on the extracted responses separation distance was adopted to capture the spread of stress across the surface of each plate. This was defined as the distance between the maximum stress points across the surface of the pieces. This distance was measured as a percentage of the diametric distance of the circular surface. This parameter was measured for the stress and deformation distributions. Secondly, area spread was also considered and is defined as the measure of the surface dominated by the highest stress and deformation values. This area was measured as a percentage of the overall plane surface. Thirdly, ratio of the area spread to the number of holes was measured, which is a metric that extends the input parameters' ability to capture stress concentration around the holes. This relates the number of holes and the local stress/deformation distribution.

All these combines to crystallize the objective of this study, to minimize stress concentration, minimize maximum stress (around the edges and otherwise), minimize maximum deformation and lastly reduces the tendency of localized deformation.

The data obtained for 50 different configurations were collected, normalized, and integrated into a single objective. All the algorithms within linear regression suite of MATLAB machine learning toolbox were tested and evaluated based on the root-mean-square error (RMSE), R-squared error (R-sq) and the quotient of these two. With respect to these, a model with a RMSE closer to zero and a R-sq closer to one is judged to perform better on prediction, and this is the basis for the metric chosen for evaluation - the quotient of R-sq and RMSE.

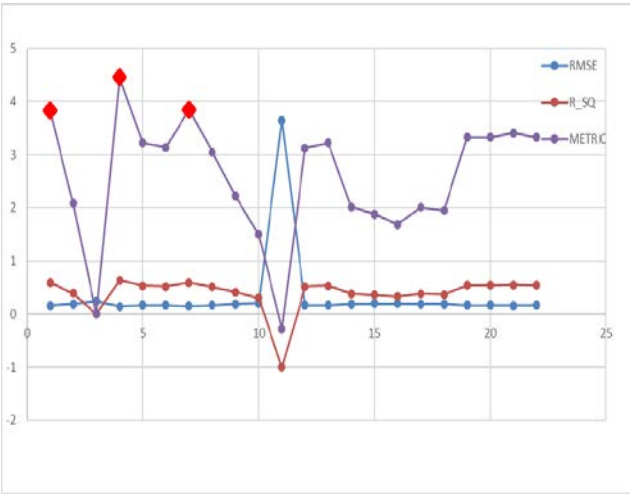

Figure 18. Comparison of regression models

As shown in the Figure 18, among the 22 models that were tested, the highest performing are models are the trees - with the best being the Boosted Ensemble Trees with the Principal Component Analysis (PCA) off. The corresponding metric here for the RMSE and R-sq are 0.143 and 0.64. The PCA feature of the regression framework basically screens out the parameters it perceives less likely to have a significant effect on the overall performance of the model. However, in this study, we see that the model performs significantly better with this feature being off. This hints at the fact that all the input parameters are relevant to a certain degree in the establishment of the results in this study. It should however be known that the objective of this study is to minimize the user-defined overall response obtained from treating the derived responses. As a result of this treatment, the output of the regression framework is interpreted such that the least values of the overall response with respect to each of the input parameters defined in Figure 19 characterizes the desired design regions.

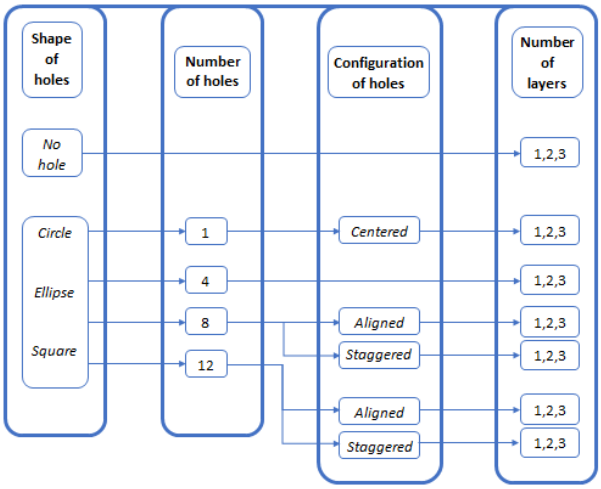

Figure 19. Relationship between level of complexities considered

The deduction from the regression framework for each of these parameters are summarized in Table 2.

Table 2. Summary of optimal behavior

Parameter	Optimal behavior/configuration
Positioning of holes	Staggered
Number of holes	8 holes
Number of plates	3 and 6 plate are identical; the use of 1 plate is highly discouraged
Shape of holes	Circular

The values presented in Table 2 are the optimal values predicted by the model selected for regression analysis. They constitute a framework that can be adopted to come up with an improved design that satisfies the study objectives as required by the specified application. It is also important to note that the overall visualization of the interplay of all the parameters concerned is somewhat difficult, as plotting on a 4 by 1 coordinate system is impractical.

3.1. Behavior and Implied Cause(s)

1. Staggard: The staggered as opposed to the aligned variation of hole placements tend to increase the space between adjacent holes as shown in Figure 20 with $\boldsymbol{d_2 > d_1}$.

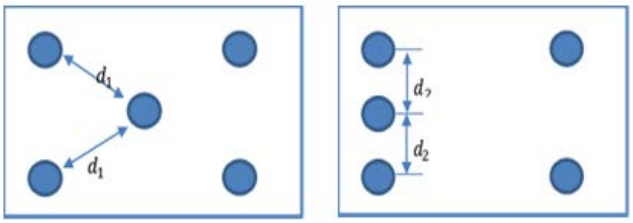

Figure 20. Comparison of staggered holes with aligned holes

The increased distance hence predisposes the specimen to a reduced density of hole distribution, therefore reducing the likelihood of stress concentration for the same number of holes.

2. 8 holes: Although a wider range of the number of holes can could have been tested, the numbers used in this study were taken in proportion to the hole size relative to the surface area of then plate. The better performance of eight holes compared to other numbers can be attributed to the fact that it balances the requirement for weight reduction and the reduction of stress concentration most suitably. A lower number of holes tend to lean towards more weight, while a higher number tend to make the specimen have too many blanks/holes that hence lead to stress concentration between close geometric transitions (corners).

3. 3 or 6 plates: the performance of a 3-plate configuration was observed to be identical to that of the 6-plate configuration. This probably points out the fact that a minimum number of plates is sufficient for a particular load threshold, which in this case is 5MPa.

4. Circular holes: Circular hoes were seen to perform better. This is likely due to the same reason circular plates were selected for this study - to minimize the tendency for stress concentration due to sudden geometric transitions. However, it should be noted that alternative orientations of the elliptical configuration were not examined. The peripheral outline of the ellipse is such that it can be changed with respect to each other as shown in Figure 21.

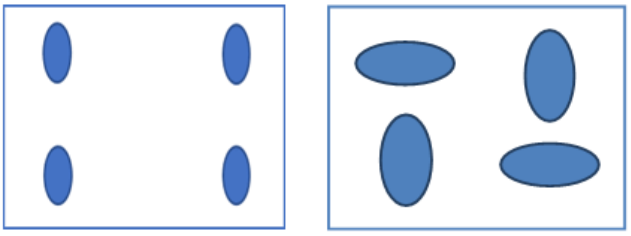

Figure 21. Comparison of orientations for elliptical holes

The results obtained for the simulation of dog bone material is presented in this section. It gives additional information on the effect of pressure on the material. For all the samples considered, the pressure of 15 Pa was assigned on the surface of the material and corresponding values of stress, strain and deformation were recorded. Table 3 shows a brief result for pressure assigned on a specimen without hole. Figure 22a - Figure 22c shows the GUI display for equivalent stress, equivalent strain, and total deformation.

Table 3. No holes at pressure of 15 Pa

S/N	Property Under Test	Definition of Property and how it is measured	Measurement
1	Equivalent von-Misses stress	The von Misses stress a metric of measurement to determine whether the structure has started to yield at any point. The stresses calculated at any point can be mathematically written into a scalar quantity known as von Misses stress, which can then be compared with experimentally observed yield points.	674.22 Pa
2	Equivalent strain	The equivalent elastic strain is defined as the limit for the values of strain up to which the object will rebound and come back to the original shape upon the removal of the load.	3.5619 x 10-8 m/m
3	Total deformation	Total deformation in this case refers to the change in size or shape of the specimen due to the application of force. The deformation is proportional to the stress applied within the elastic limits of the material.	9.517 x 10-11 m

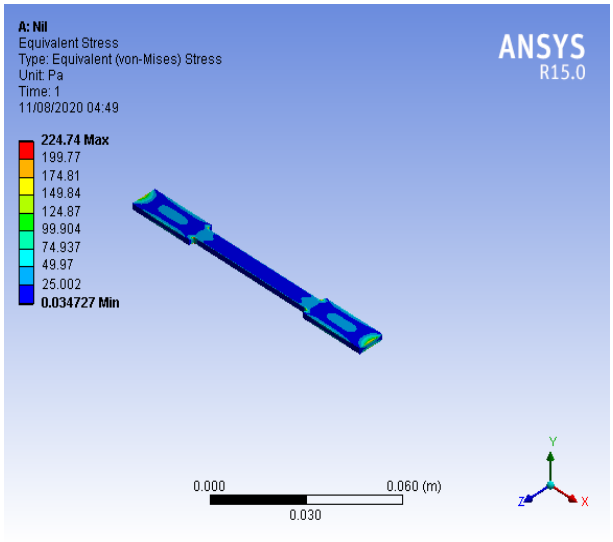

Figure 22a. Equivalents stress on dog bone

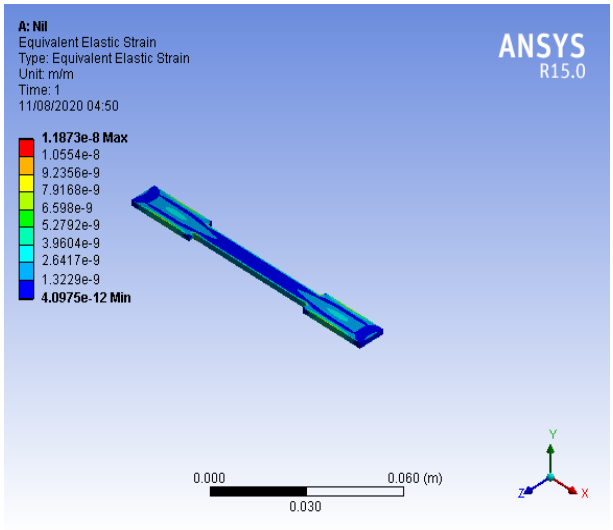

Figure 22b. Equivalents strain on dog bone

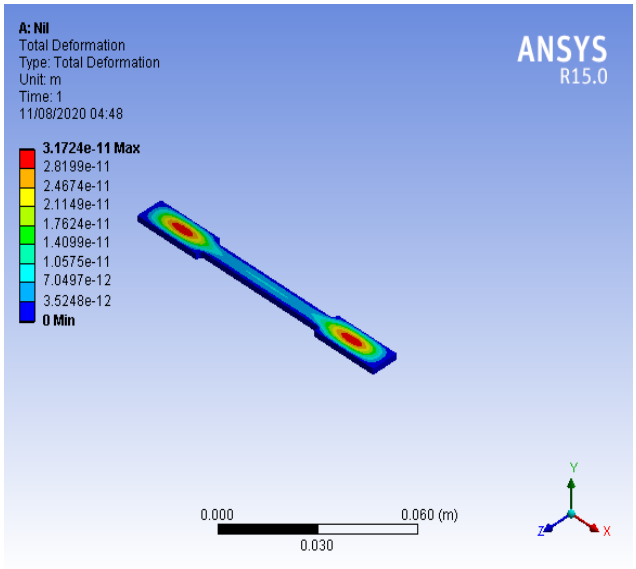

Figure 22c. Total deformation dog bone

3.2. Increasing Holes Diameter

Figure 23 present the result from determination of effect of holes in dog bone by observing the maximum equivalent (von-Misses) stress measurement. From Figure 23, the value of equivalent stress measured does vary uniformly by continuous increase or decrease, but rather it moves in a zigzag pattern. Although the zigzag pattern still moves in slight decreasing manner.

Figure 24 shows variation of equivalent stress with hole diameter for single hole. Result in this section is from determination of effect of hole in dog bone by observing the maximum equivalent elastic strain measurement. The behavior from the graph observed here is like that of Figure 24 for equivalent stress. But in this case, continuous decrease in equivalent strain value was observed from no hole to 2 mm hole, after which the value continues to increase.

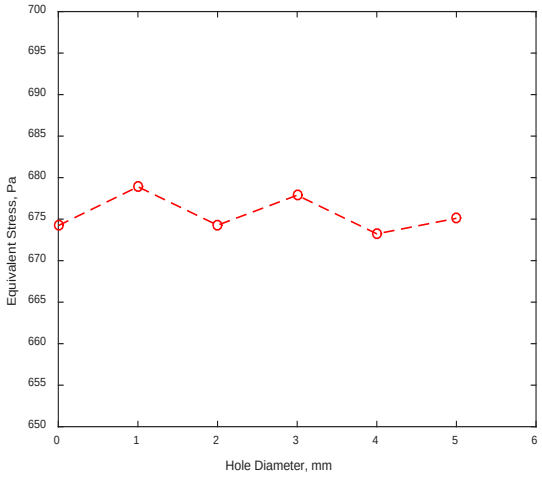

Figure 23. Equivalent Stress vs Hole diameter

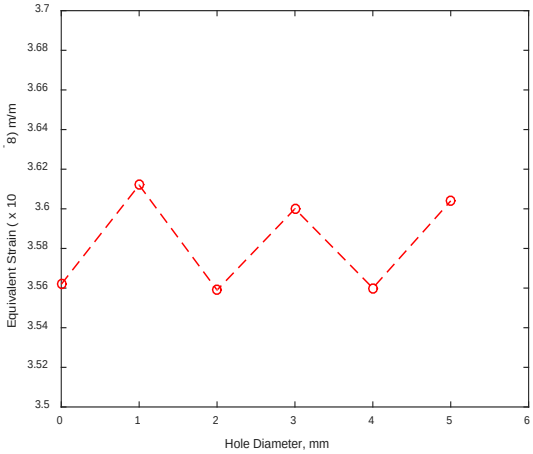

Figure 24. Equivalent Strain vs Hole diameter

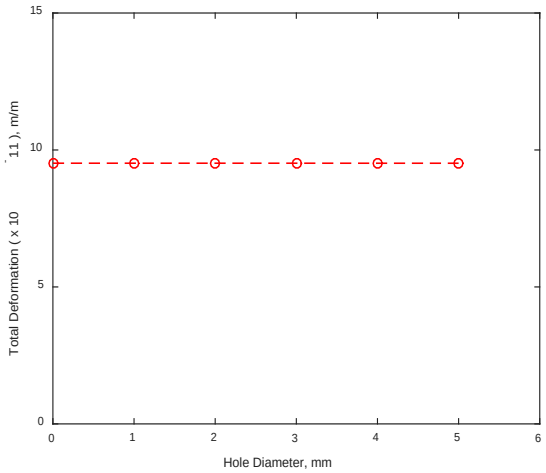

Figure 25. Total deformation vs Hole diameter

Result in this section is from determination of effect of holes in dog bone by observing the maximum total deformation measurement and is presented in Figure 25. Unlike the pattern of variation observed for the equivalent stress and equivalent strain, there is no significant change in the value of maximum total deformation for specimen without hole and with hole (all five-hole diameters).

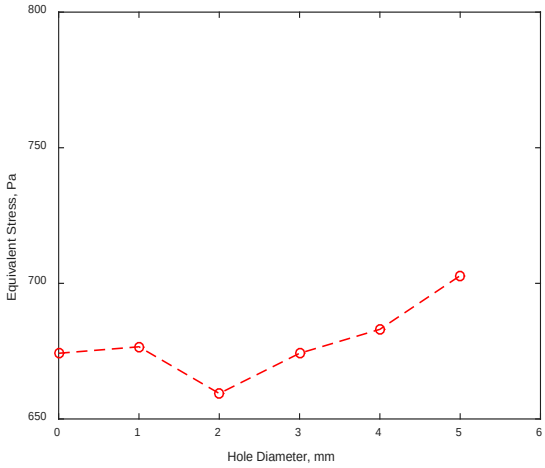

Figure 26. Equivalent Stress vs Hole diameter

3.3. Five Holes

Result in this section is from determination of effect of multiple (5) holes in dog bone by observing the maximum equivalent (von-Misses) stress measurement. From Figure 26, the value of equivalent stress measured slightly increase for increase when the hole diameter is 1 mm, then it decreases with 2 mm diameter. But further increase the hole diameter from 3 mm to 5 mm, show continues increase in the equivalent stress value.

Figure 27 shows variation of equivalent stress with hole diameter for multiple (5) holes. Result in this section is from determination of effect of five (5) holes in dog bone by observing the maximum equivalent elastic strain measurement. The behavior from the graph observed here is like that of Figure 26 for equivalent stress. But in this case, continuous decrease in equivalent strain value was observed from no hole to 2 mm hole, after which the value continues to increase

Result in this section is from determination of effect of multiple (5) holes in dog bone by observing the maximum total deformation measurement and is presented in Figure 28. It can be observed from the figure that there is no change in the value of total deformation for all the hole diameters considered.

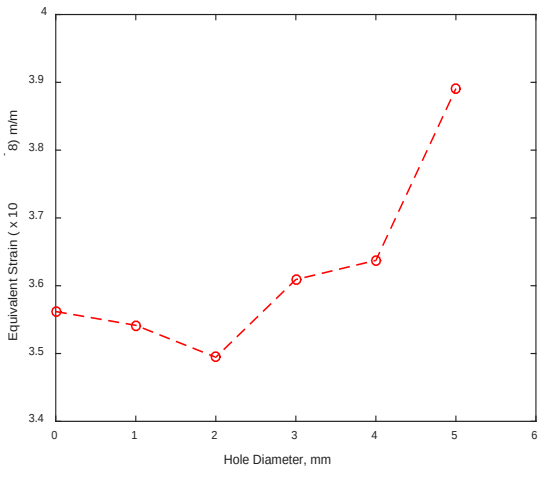

Figure 27. Equivalent Strain vs Hole diameter

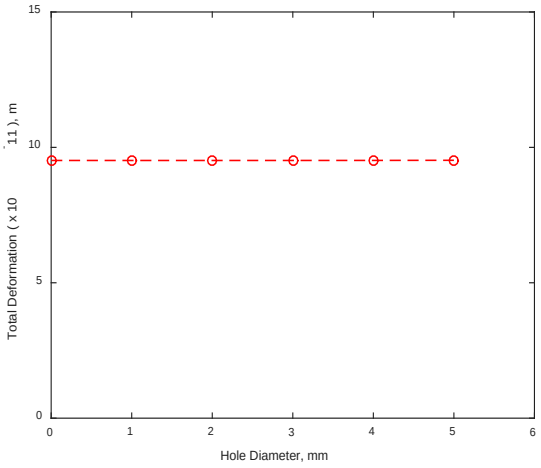

Figure 28. Total Deformation vs Hole diameter

4. Conclusion

Effect of pressure on composite material using finite element method had been studied in this work. This was measured in terms of equivalent stress, equivalent strain and total deformation on the material for different shapes and configurations. Circular shape and dog bone, both without holes were the shapes considered as initial or primary configuration. For the circular shape, single layer and multiple layers were studied, hole perforated on specimens were studied, number and holes and different shapes of holes were also studied. The optimal behavior predicted for the circular shape specimen suggest that staggered arrangement, 8 holes, 3 or 6 layers of plate combined, and circular holes will be the required combination for best performance. This deduction was made based on the prediction by the model selected for regression analysis. In the case of dog bone shape, no hole, single hole, and multiple holes were considered. It was observed that multiple (5) holes with 5 mm will significantly increase the equivalent stress and equivalent strain on the specimen, while no significant change was observed for the total deformation. On generalized perspective, hole diameter of 2 mm is favorable as compared to the remaining hole diameter considered in this study both in terms of strength and weight reduction.

References

[1] F. C. Campbell: *Structural Composite Materials*, Chapter 1: Introduction to Composite Materials; ASM International, 2010.

[2] P. D. Pastuszak; A. Muc: *Application of Composite Materials in Modern Construction*, Key Engineering Materials, 542, 2013, pp 119-129.

[3] E. C. Botelho; R. A. Silva; L. Z. Pardini; M. C. Rezende: *A Review on the Development and Properties of Continuous Fibre/epoxy/aluminium Hybrid Composites*, Journal of Materials Research, 9(3), 2016, pp 247-256.

[4] H. Birch: *Changing Planes*, Aerospace Materials. www.chemistryworld.org (October Issue), 2011.

[5] A. F. Avila; P. O. Bueno: *An experimental and numerical study on adhesive joints for composites*. Composite Structures 64, 2004, 531-537.

[6] Z. Qin; K. Yang; J. Wang; L. Zhang; J. Huang; H. Peng; J. Xu: *The effects of geometrical dimensions on the failure of composite-to-composite adhesively bonded joints*. The Journal of Adhesion, 2020.

[7] D. Zhou; M. Di: *Numerical Simulation Analyses of Single Lap Joints for Wood-PE Composites Formed with Epoxy and Acrylic Ester Adhesives*. BioResources 14(3), 2019, 5908-5922.

[8] Department of the Army, U.S. Army Corps of Engineers, Washington DC 20314-1000*: Engineering and Design of Composite Materials fir Civil Engineering Structures*, Technical Letter No. 1110-2-548, 1997.

[9] M. Arif; M. Aisf; I. Ahmed*: Advanced Composite Materials for Aerospace Applications - a Review*, International Journal of Engineering and Manufacturing Science, 7(2), 2017, pp 393-409.

[10] R. B. Deo; J. H. Starnes Jr.; R. C. Holzwarth: *Low-Cost Composite Materials and Structures for Aircraft Applications*, Paper presented at the RTO AVT specialist meeting on "Low Cost Composite Structures", Leon, Norway; May 7-11 May 2001. Published in RTO-MP-069(II), 2001.

[11] F. Rubino; A. Nistico; F. Tucci; P. Carlone: *Marine Application of Fibre Reinforced Composites: A Review*, Journal of Marine Science and Engineering, 8(6), 2020.

[12] R. A. Shenoi; J. D. Barton; S. Quinn; J. I. R. Blake: *Composite Materials for Marine Applications - Key Challenges for the Future*. 2011.